

Cooperative Ordering of Gapped and Gapless Spin Networks in $\text{Cu}_2\text{Fe}_2\text{Ge}_4\text{O}_{13}$

T. Masuda,^{1,*} A. Zheludev,¹ B. Grenier,² S. Imai,^{3,†} K. Uchinokura,^{3,‡} E. Ressouche,² and S. Park⁴

¹Condensed Matter Science Division, Oak Ridge National Laboratory, Oak Ridge, Tennessee, 37831-6393, USA

²CEA-Grenoble, DRFMC / SPSMS / MDN, 17 rue des Martyrs, 38054 Grenoble, Cedex, France

³Department of Advanced Materials Science, University of Tokyo, 5-1-5, Kashiwa-no-ha, Kashiwa, 277-8581, Japan

⁴NIST Center for Neutron Research, National Institute of Standards and Technology, Gaithersburg, Maryland, 20899, USA

(Received 20 April 2004; published 9 August 2004)

The unusual magnetic properties of a novel low-dimensional quantum ferrimagnet $\text{Cu}_2\text{Fe}_2\text{Ge}_4\text{O}_{13}$ are studied using bulk methods, neutron diffraction, and inelastic neutron scattering. It is shown that this material can be described in terms of two low-dimensional quantum spin subsystems, one gapped and the other gapless, characterized by two distinct energy scales. Long-range magnetic ordering observed at low temperatures is a cooperative phenomenon caused by weak coupling of these two spin networks.

DOI: 10.1103/PhysRevLett.93.077202

PACS numbers: 75.10.Jm, 75.25.+z, 75.50.Ee

In low-dimensional magnets, quantum spin fluctuations are often potent enough to completely destroy long-range order even at zero temperature. Quantum disorder in systems with a spin gap, also known as “quantum spin liquids,” is particularly robust. These systems resist “spin freezing,” i.e., forming a magnetically ordered state, even in the presence of weak 3-dimensional (3D) interactions or magnetic anisotropy. In contrast, gapless low-dimensional magnets have a quantum-critical ground state and, being extremely sensitive to any external perturbations, can be forced to order more easily. Either way, when quasi-low-dimensional magnets *do* order, it typically involves some interesting and exotic physics. For example, spin freezing may be induced by *nonmagnetic* [1,2] or magnetic [3] impurities, or by a Bose-condensation of magnons induced by an external magnetic field [4–6].

An alternative ordering mechanism can be envisioned in a complex material that incorporates two intercalated low-dimensional subsystems. Particularly interesting are cases involving a mixture of gapless and gapped entities. If these two spin networks were totally isolated from one another, they would remain disordered at any $T > 0$, due to their reduced dimensionality [7]. However, arbitrary weak interactions between the two subsystems can drastically change this outcome. Divergent one- or two-dimensional correlations in the gapless subsystem, combined with short-range correlations in the third direction propagated by the subsystem with a gap, will ultimately coalesce into a 3D ordered phase at a finite temperature. Provided that interactions between the two subsystems are relatively weak, this new *cooperative ordered state* can be expected to possess some rather unique characteristics. Among these are a strong quantum suppression of ordered moments in the nominally gapped subsystem, a coexistence of conventional spin waves and remanent gap modes, interactions, and “anticrossing” between such excitations, *etc.* In the present Letter we report an experi-

mental realization and study of this novel cooperative ordering mechanism in the quantum ferrimagnet $\text{Cu}_2\text{Fe}_2\text{Ge}_4\text{O}_{13}$.

The crystal structure of $\text{Cu}_2\text{Fe}_2\text{Ge}_4\text{O}_{13}$ [8] can be viewed as a modification of that of the famous spin-Peierls compound CuGeO_3 [9]. It consists of three distinct components: “crankshaft”-shaped chains of edge sharing FeO_6 octahedra, Cu-O-Cu dimers, and oligomers of four GeO_4 tetrahedra [8]. The mutual arrangement of these structural elements is visualized in Fig. 1(a) and 1(b). The space group is monoclinic, $P2_1/m$, with lattice parameters $a = 12.101$, $b = 8.497$, $c = 4.869$, and $\beta = 96.131^\circ$. Fe^{3+} and Cu^{2+} carry $S = 5/2$ and $S = 1/2$, respectively. The crankshaft FeO_6 chains run along the b axis. They are linked by GeO_4 tetrahedra in c direction and by Cu^{2+} dimers in the a direction. A plausible network of superexchange pathways is shown in Fig. 1(c). The key piece of information required to understand the magnetism of $\text{Cu}_2\text{Fe}_2\text{Ge}_4\text{O}_{13}$ is the hierarchy of the corresponding exchange constants. Knowing this hierarchy will allow us to formulate the model in terms of spin “chains,” “planes,” and “dimers.”

Single crystals of $\text{Cu}_2\text{Fe}_2\text{Ge}_4\text{O}_{13}$ were grown in O_2 atmosphere by floating zone method and were characterized using bulk magnetic susceptibility and heat capacity measurements. The $\chi(T)$ curves measured using a commercial SQUID magnetometer in an $H = 1000$ Oe magnetic field applied perpendicular and parallel to $\{110\}$ plane are plotted in open symbols in Fig. 2(a). These data are characteristic of a quasi-low-dimensional antiferromagnet: the development of broad maximum at $T \sim 100$ K is followed by an antiferromagnetic phase transition at $T_N = 39$ K. This transition is also manifest in the heat capacity data shown in Fig. 2(b) and is the only prominent feature in our temperature range.

As a “zeroth approximation,” the measured susceptibility was fit to a sum of two contributions calculated for isolated $S = 5/2$ chains [10] and $S = 1/2$ dimers. The

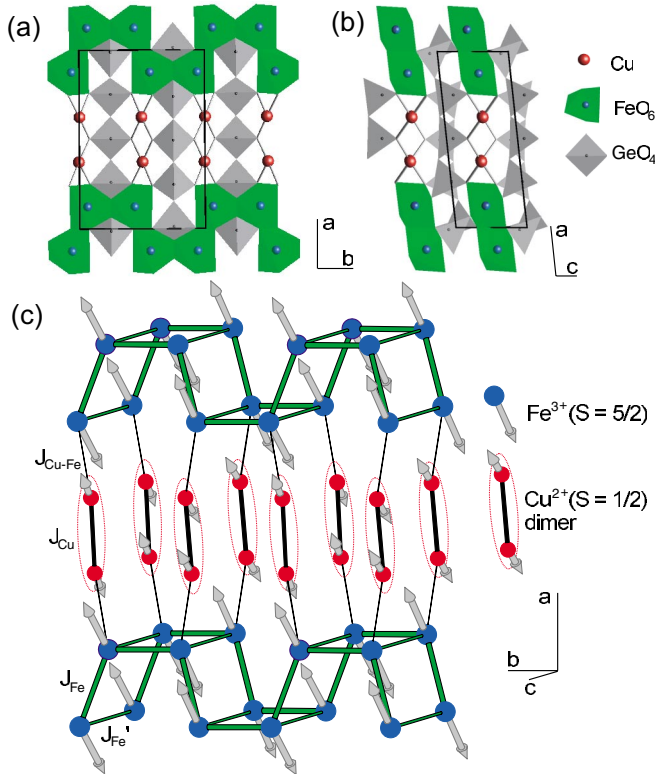


FIG. 1 (color). (a) and (b) Crystal structure of $\text{Cu}_2\text{Fe}_2\text{Ge}_4\text{O}_{13}$ projected onto (a, b) and (a, c) crystallographic planes. (c) Magnetic structure and possible exchange pathways in $\text{Cu}_2\text{Fe}_2\text{Ge}_4\text{O}_{13}$.

best fit is obtained assuming the Cu-Cu and Fe-Fe exchange constants to be $J_{\text{Cu}} = 25$ MeV and $J_{\text{Fe}} = 1.7$ MeV, respectively. The average gyromagnetic ratio of Cu^{2+} and Fe^{3+} is determined to be $g = 2.04$ by room-temperature ESR measurements. The result of the fit is shown in a solid line in Fig. 2, with the dashed and dotted lines representing the Fe chain and Cu dimer components, correspondingly. Though rather crude, this simple analysis gives us a rough idea of the magnitude of the relevant exchange constants.

The spin arrangement in the magnetically ordered state was determined by neutron diffraction experiments on the CRG-D23 lifting-counter diffractometer at Institute of Laue Langevin. 338 nuclear and 222 magnetic independent reflections were collected at $T = 1.5$ K using a 0.3 g sample. The results unambiguously indicate an almost antiparallel and slightly canted spin structure with all spins predominantly in (a, c) crystallographic plane, as shown in Fig. 1(c). The propagation vector is $(0, 0, 0.5)$. The most important result pertains to the magnitudes of the ordered moments: $m_{\text{Cu}} = 0.38(4)\mu_{\text{B}}$ and $m_{\text{Fe}} = 3.62(3)\mu_{\text{B}}$. The moment's orientations in the standard Cartesian coordinate system linked to the crystallographic unit cell were found to be $\mathbf{m}_{\text{Cu}} = (-0.227, 0.035, -0.301)\mu_{\text{B}}$ and $\mathbf{m}_{\text{Fe}} = (2.163, 0.121, 2.892)\mu_{\text{B}}$, respectively. The temperature

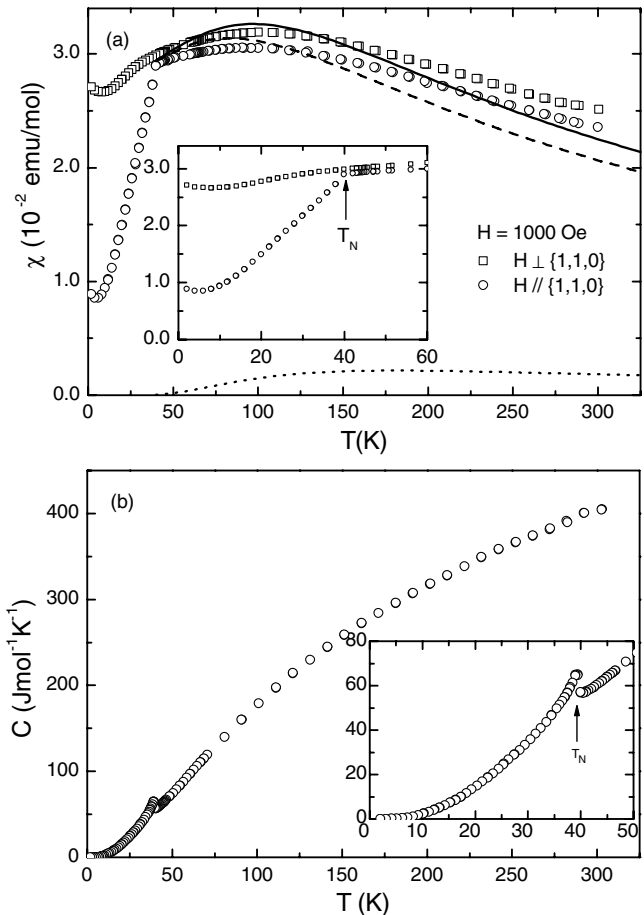


FIG. 2. (a) Magnetic susceptibility of $\text{Cu}_2\text{Fe}_2\text{Ge}_4\text{O}_{13}$ measured in field applied perpendicular and parallel to cleaved plane (symbols). Solid, dashed and dotted lines are explained in the text. (b) Heat capacity of $\text{Cu}_2\text{Fe}_2\text{Ge}_4\text{O}_{13}$ in zero field.

dependence of the magnetic structure was deduced from the behavior of $(2\ 1\ -0.5)$, $(0\ 2\ 0.5)$, $(-1\ 1\ 0.5)$, and $(-2\ 1\ 1.5)$ Bragg reflections. The evolution of sublattice moments for Fe^{3+} and Cu^{2+} are shown in the main panel of Fig. 3. They were determined under the assumption that all spin orientations are T -independent.

The observed antiparallel spin arrangement indicates that all the exchange constants in our model for $\text{Cu}_2\text{Fe}_2\text{Ge}_4\text{O}_{13}$ are antiferromagnetic (Fig. 1). Our main finding, however, is the drastic suppression of the ordered moments on the Cu^{2+} sites, as compared to their classical expectation value of $1\mu_{\text{B}}$. To explain this behavior we have to assume that the Cu dimers are effectively isolated from the rest of the system and become only partially polarized by the long-range order on the Fe sites. In other words, $J_{\text{Cu}} \gg J_{\text{Cu-Fe}}$, and the Cu^{2+} moments are reduced due to strong *local* quantum spin fluctuations within the dimers. The suppression of the Fe^{3+} moment is less pronounced. This is undoubtedly due to the large value of the Fe^{3+} spin and allows us to regard the Fe subsystem as a semiclassical one. The observed small canting of the spin

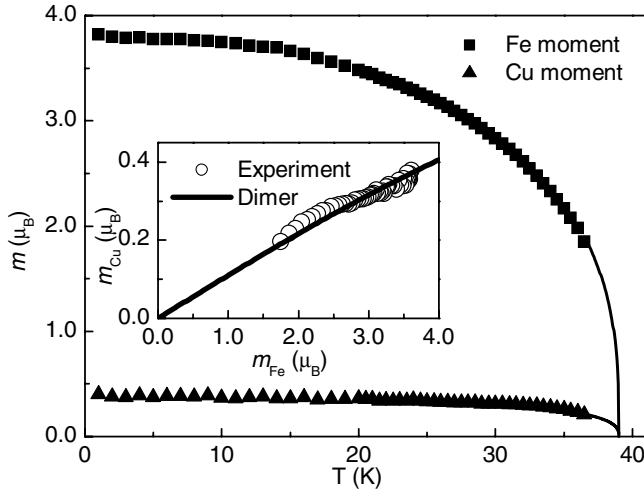


FIG. 3. Measured temperature dependence of the Fe^{3+} - and Cu^{2+} -ordered moments (main panel). Inset: ordered moment on the Cu^{2+} sites plotted vs. that on Fe^{3+} . The solid line is a fit to the staggered magnetization curve for an isolated dimer.

structure can be attributed to Dzyaloshinskii-Moriya interactions and other insignificant anisotropy effects.

The strongly dimerized nature of the Cu^{2+} spins has one interesting consequence. At the Mean Field level, if each dimer is treated as single inseparable entity, the ordered moment on the Cu sites is seen as being *induced* by an effective external staggered exchange field. It is determined by the staggered magnetization function $M_{+-}(H_{+-}, T)$ for an isolated dimer. Excluding direct interdimer interactions, the exchange field H_{+-} is proportional to the ordered moment on the Fe subsystem, *regardless* of the internal network of the latter. Assuming that $k_B T \ll J_{\text{Cu}}$, $M_{+-}(H_{+-}, T) \approx M_{+-}(H_{+-}, 0) \equiv M_{+-}^{(0)}(H_{+-})$. This establishes a unique relation between m_{Cu} and m_{Fe} :

$$m_{\text{Cu}} = M_{+-}^{(0)}(\alpha m_{\text{Fe}}), \quad (1)$$

where $\alpha \sim J_{\text{Cu-Fe}}$ is the effective Mean Field coupling constant. For $\text{Cu}_2\text{Fe}_2\text{Ge}_4\text{O}_{13}$, this relation indeed holds very well, as shown in the inset of Fig. 3. Here the solid line is a best fit of Eq. (1) to the experimental data obtained with $J_{\text{Cu-Fe}}/J_{\text{Cu}} = 0.11$.

While the Cu subsystem appears to be well described as a collection of dimers, the network of Fe^{3+} spins is considerably more complicated, with several possible interaction pathways in the (b, c) plane. To better understand these interactions, we performed a series of inelastic neutron scattering experiments that probed the low-energy spin excitation spectrum. The data were collected for energy transfers of up to 10 meV using the SPINS cold 3-axis spectrometer installed at the National Institute of Standards and Technology and the HBI thermal 3-axis spectrometer at the High Flux Isotope Reactor at Oak Ridge National Laboratory. Two coaligned single crystal

samples had a total mass of 3.5 g. Several configurations were exploited, with final neutron energies of 5 meV, 3 meV, or 13.5 meV, with several settings of the sample relative to the scattering plane. A detailed report of these measurements will be published elsewhere, and only the main results will be summarized here.

Sharp spin wave excitations of resolution-limited energy width were observed at all wave vectors, as illustrated by typical scans shown in Fig. 4(b). At least two separate excitation branches are present. Their dispersion along the a^* direction was undetectable in our experiments. In contrast, the dispersion along the b^* and c^* reciprocal-space axes is quite pronounced. The measured dispersion curves are plotted in symbols in Fig. 4(a). These low-energy data can be explained by conventional spin wave theory for a 2-dimensional network that includes only the Fe^{3+} spins, and direct Fe-Fe exchange interactions shown in Fig. 1 [11]. Dispersion curves for this model were calculated as explained in Ref. [12]. With eight Fe^{3+} ions per magnetic unit cell there are actually four two-fold degenerate spin wave branches. Because of particular values of the 3D magnetic unit cell structure factors, only two modes produce strong contributions at a time for each of the scans shown. An excellent fit to the data is obtained assuming $J_{\text{Fe}} = 1.60(2)$ meV and $J'_{\text{Fe}} = 0.12(1)$ meV, and assuming a small empirical anisotropy gap $\Delta = 2.02(40)$ meV. The result of the fit is shown in solid lines in Fig. 4(a). The obtained value of J_{Fe} is consistent with our previous estimate based on simple-minded fits to magnetic susceptibility data. We conclude that the Fe layers are indeed to be viewed as chains running along the b crystallographic axis, with only weak interchain coupled along the c direction.

The fact that the low-energy excitations are entirely due to the Fe^{3+} moments confirms the main idea behind our “two-subsystem” model for $\text{Cu}_2\text{Fe}_2\text{Ge}_4\text{O}_{13}$. The key point is that $J_{\text{Fe-Cu}}, J_{\text{Fe}} \ll J_{\text{Cu}}$. As previously explained in Ref. [3] for the case of R_2BaNiO_5 nickelates, such a hierarchy of exchange constants leads to a *separation of energy scales* of magnetic excitations. The Cu centered (dimer) excitations are confined to high frequencies, while low frequencies are entirely dominated by “acoustic” fluctuations of the Fe^{3+} spins. However, the coupling between the two subsystems *can not be ignored*: it is essential for completing a 3D network of magnetic interactions and enabling long-range magnetic ordering at a finite temperature. At low frequencies the dimers can be integrated out and replaced by an effective interaction J_{eff} between Fe^{3+} spins along the a axis. Since the staggered susceptibility of each Cu dimer is proportional to $1/J_{\text{Cu}}$, we can estimate $J_{\text{eff}} \propto J_{\text{Fe-Cu}}^2/J_{\text{Cu}}$. The absence of spin wave dispersion along the a axis can thus be explained either by the weakness of $J_{\text{Fe-Cu}}$ that couples the two subsystems, or by the large value of J_{Cu} .

To summarize, our experiments reveal the unconventional *cooperative* ordering of the low-dimensional quan-

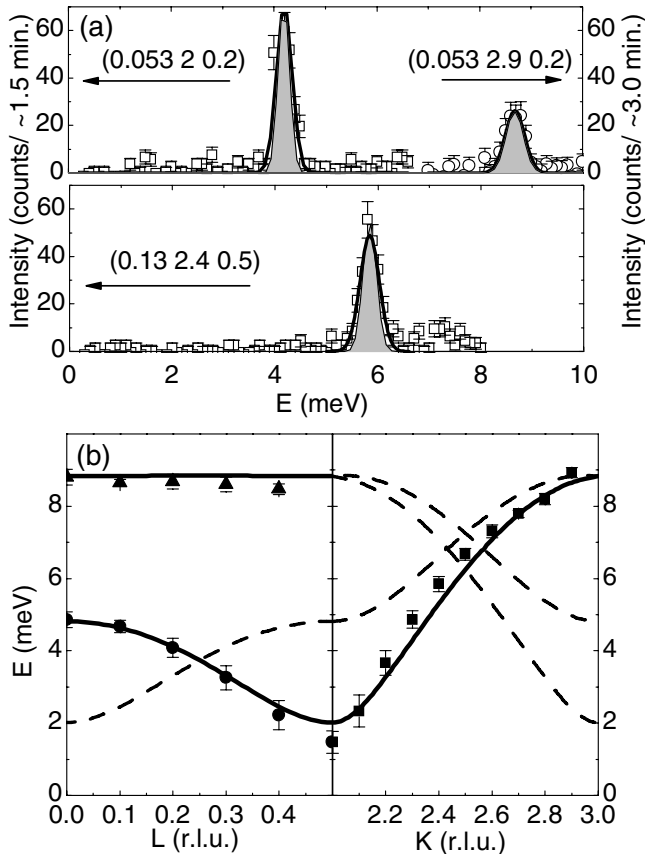


FIG. 4. (a) Typical constant- q scans collected in $\text{Cu}_2\text{Fe}_2\text{Ge}_4\text{O}_{13}$ at $T = 1.4$ K for different wave vectors. Shaded Gaussian curves represent the experimental energy resolution. Solid lines are Gaussian fits to the data. (b) Measured dispersion of low-energy spin waves in $\text{Cu}_2\text{Fe}_2\text{Ge}_4\text{O}_{13}$ (symbols). Lines represent spin wave theory fits to the data as described in the text.

tum spin subsystems of $\text{Cu}_2\text{Fe}_2\text{Ge}_4\text{O}_{13}$ and the persistence of quantum spin fluctuations even in the 3D-ordered phase. A very interesting remaining issue is that of Cu^{2+} -centered excitations in this material, expected to occur at higher energy transfers: what happens to the triplet dimer modes when long-range order sets in? In the context of separation of energy scales, they may be expected to survive in the ordered state. In this case, at least one member of the triplet will have *longitudinal* polarization, and therefore be totally incompatible with conventional spin wave theory. Another exciting avenue for future studies are other members of the hypothetical family of compounds with the general formula $\text{Cu}_{n-2}\text{Fe}_2\text{Ge}_n\text{O}_{3n+1}$ [8]. In these species, the Fe layers

alternate with layers of Cu oligomers of length $n - 2$. Cooperative ordering can be expected in all these materials, but should be qualitatively different in even- n and odd- n members, where the Cu subsystem is either gapped and gapless, respectively.

We thank Dr. Chakoumakos for crystal structure analysis in the early stage of this study. Work at ORNL was carried out under Contract No. DE-AC05-00OR22725, U.S. Department of Energy. Experiments at NIST were supported by the NSF through Grants No. DMR-0086210 and No. DMR-9986442. Work in Japan was supported in part by a Grant-in-Aid for COE Research "SCP Coupled System" from the Ministry of Education, Science, Sports and Culture of Japan.

*Electronic address: masudat@ornl.gov

[†]Present address: Optical Device Dept. R & D Divisions, The Furukawa Electronic Co., Ltd. 2-4-3, Okano, Nishiku, Yokohama, Kanagawa, 220-0073, Japan

[‡]Present address: The Institute of Physical and Chemical Research (RIKEN), Wako, Saitama 351-0198, Japan

- [1] M. Hase, I. Terasaki, Y. Sasago, K. Uchinokura, and H. Obara, Phys. Rev. Lett. **71**, 4059 (1993).
- [2] Y. Uchiyama, Y. Sasago, I. Tsukada, K. Uchinokura, A. Zheludev, T. Hayashi, N. Miura, and P. Böni, Phys. Rev. Lett. **83**, 632 (1999).
- [3] A. Zheludev, S. Maslov, T. Yokoo, S. Raymond, S. E. Nagler, and J. Akimitsu, J. Phys. Condens. Matter **13**, R525 (2001).
- [4] Z. Honda, H. Asakawa, and K. Katsumata, Phys. Rev. Lett. **81**, 2566 (1998).
- [5] A. Oosawa, M. Ishii, and H. Tanaka, J. Phys. Condens. Matter **11**, 265 (1999).
- [6] Y. Chen, Z. Honda, A. Zheludev, C. Broholm, K. Katsumata, and S. M. Shapiro, Phys. Rev. Lett. **86**, 1618 (2001).
- [7] N. D. Mermin and H. Wagner, Phys. Rev. Lett. **17**, 1133 (1966).
- [8] T. Masuda, B. C. Chakoumakos, C. L. Nygren, S. Imai, and K. Uchinokura, J. Solid State Chem. **176**, 175 (2003).
- [9] M. Hase, I. Terasaki, and K. Uchinokura, Phys. Rev. Lett. **70**, 3651 (1993).
- [10] M. E. Fisher, Am. J. Phys. **32**, 343 (1964).
- [11] Because of a small alternation in bond length, the coupling constant J_{Fe} may actually slightly alternate from one bond to the next. This alternation is apparently too weak to affect the dispersion relations measured in this work, and was thus not included in the spin wave calculation.
- [12] A. W. Sáenz, Phys. Rev. **125**, 1940 (1962).